

# Hyperpolarized [1-<sup>13</sup>C]pyruvate Magnetic Resonance Spectroscopic Imaging (MRSI) identifies pancreatic cancer subtypes in mice

Irina Heid<sup>1</sup>, Moritz Mayer<sup>1</sup>, Katja Peschke<sup>2</sup>, Geoffrey J. Topping<sup>3</sup>, Katja Steiger<sup>4</sup>, Martin Grashel<sup>3</sup>, Maximilian Aigner<sup>3</sup>, Marija Trajkovic-Arsic<sup>5</sup>, Maximilian Reichert<sup>2</sup>, Franz Schilling<sup>3</sup>, Rickmer Braren<sup>1,6</sup>

<sup>1</sup> Technical University of Munich, Institute of Diagnostic and Interventional Radiology, School of Medicine, Klinikum rechts der Isar, Munich, Germany

<sup>2</sup> Technical University of Munich, Internal Medicine II, Klinikum rechts der Isar, Munich, Germany

<sup>3</sup> Technical University of Munich, Department of Nuclear Medicine, School of Medicine, Klinikum rechts der Isar, Munich, Germany

<sup>4</sup> Technical University of Munich, Institute of Pathology, School of Medicine, Munich, Germany

<sup>5</sup> West German Cancer Center, University Hospital Essen, Division of Solid Tumor Translational Oncology, German Cancer Consortium (DKTK), partner site Essen, Essen, Germany

<sup>6</sup> German Cancer Consortium (DKTK), Partner Site Munich, Munich, Germany

## Introduction

Pancreatic ductal adenocarcinoma (PDAC) is a heterogeneous disease with poor prognosis in need of non-invasive subtype biomarkers. Two main transcriptional subtypes have been identified: Classical and quasi-mesenchymal (QM)<sup>1</sup>. The QM subtype is associated with increased glucose metabolism<sup>2,3</sup>, high expression of monocarboxylate transporter 4 (MCT4)<sup>4,5</sup> and can possibly be detected by metabolic imaging. We here present hyperpolarized (HP)-[1-<sup>13</sup>C]pyruvate chemical-shift imaging (CSI) in combination with Diffusion-Weighted Imaging (DWI) for QM subtype prediction in endogenous murine (m)PDAC.

## Methods

**Subjects:** 24 *Ptf1a<sup>Cre/wt</sup>;LSL-KRAS<sup>G12D/wt</sup>;Tp53<sup>fl/fl</sup>* tumor mice, 29 distinct tumor nodules.

**MR System:** 7T MRI (Bruker/Agilent) with a dual-tuned <sup>1</sup>H/<sup>13</sup>C 31mm volume coil.

**Proton Imaging:** T<sub>2</sub>-weighted anatomical RARE, DWI (0.25x0.25x1mm<sup>3</sup>; 12 b-values 12-1500 s/mm<sup>2</sup>).

**<sup>13</sup>C Imaging:** multi-frame single-slice axial 2D phase encoded CSI (2x2x3mm, TR=5s) with hyperpolarized [1-<sup>13</sup>C]pyruvate (80mM).

**Histology:** Tumors were removed, formalin fixed, paraffin embedded, cut aligned to the axial imaging plane and histologically processed (H&E, MCT4).

**Cytology:** Four cell lines were isolated from distinct tumor nodules, cultured under standard conditions (DMEM, 5mM glucose), processed and stained for Vimentin, MCT4, DAPI (Leica Confocal Microscope).

**Analysis:** Data was analyzed using MATLAB and GraphPad Prism 7.0.

## Results/Discussion

We observed high heterogeneity in the *in vivo* metabolic signal of complex endogenous mPDAC compared to orthotopically implanted mPDAC tumors derived from established murine cell lines<sup>5</sup>. Ratios of the area under the curves of lactate to pyruvate spectral peak time-courses (AUC<sub>l</sub>/AUC<sub>p</sub>) correlated well with the corresponding MCT4 staining (Fig. 1A-C). *In vivo* heterogeneity of AUC<sub>l</sub>/AUC<sub>p</sub> was independent of tumor

cellularity (Fig. 1D-F). Primary cells derived from AUC<sub>c</sub>/AUC<sub>p</sub><sup>high</sup> tumors (Fig. 1E, F, red) showed an elongated QM-like appearance (Fig. 2A), high Vimentin and MCT4 expression (Fig. 2B-D) and increased lactate dehydrogenase (LDH) activity *in vitro* (Fig. 2E), as compared to cuboid shaped AUC<sub>c</sub>/AUC<sub>p</sub><sup>low</sup> cells (Fig. 1E, F, blue and Fig. 2, blue). Multiparametric MRSI and DWI with HP-pyruvate may be a promising method for non-invasive detection of metabolic phenotypes and corresponding molecular subtypes in PDAC.

### Conclusions

We confirmed the link of the QM subtype and MCT4 tissue expression in murine PDAC. We further show that the QM subtype can be detected by multiparametric MRSI/DWI with HP-pyruvate. Considering the observed metabolic heterogeneity in PDAC and its association with known molecular subtypes, implementing metabolic phenotyping in clinical routine might facilitate future patient stratification and treatment monitoring.

### Acknowledgement

We thank Irina Skuratovska and Marion Mielke for excellent technical support in this project. We acknowledge support from the Deutsche Forschungsgemeinschaft (DFG, German Research Foundation - 391523415, SFB 824).

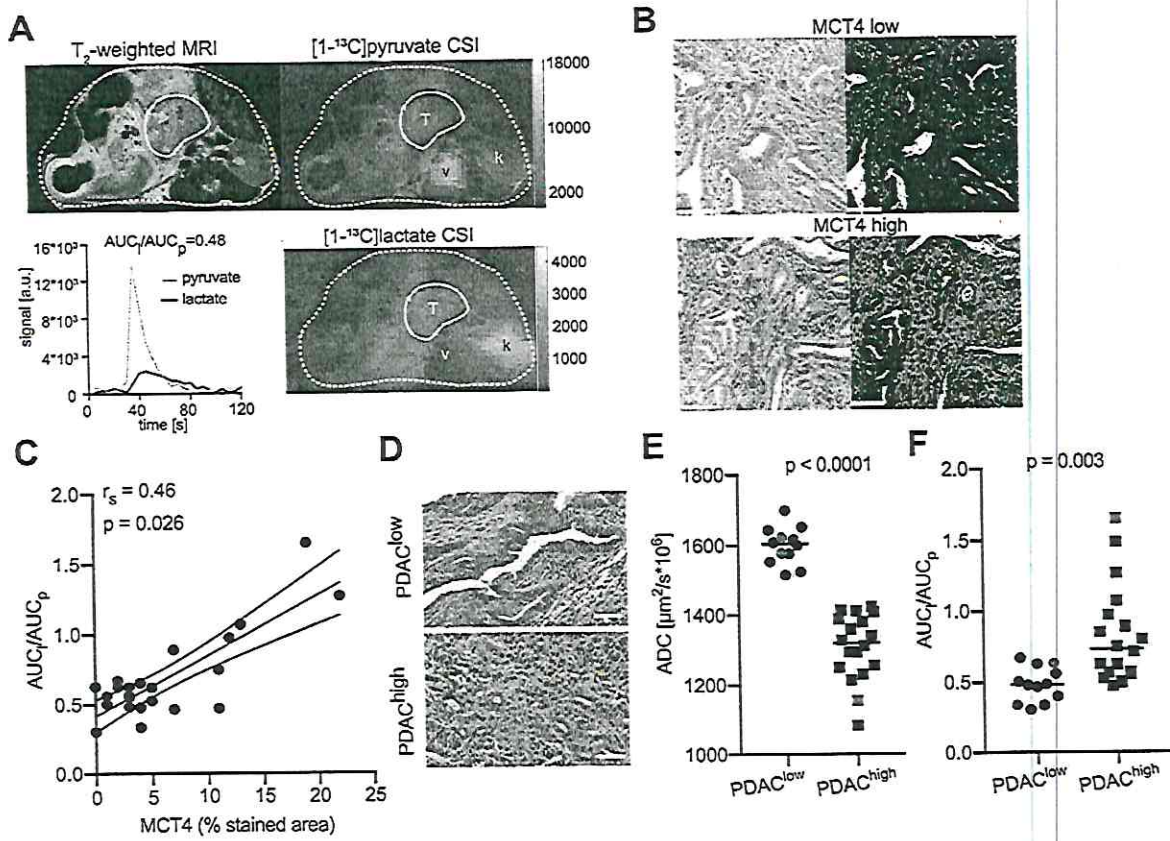
### Disclosure

I or one of my co-authors have no financial interest or relationship to disclose regarding the subject matter of this presentation.

#### Affix

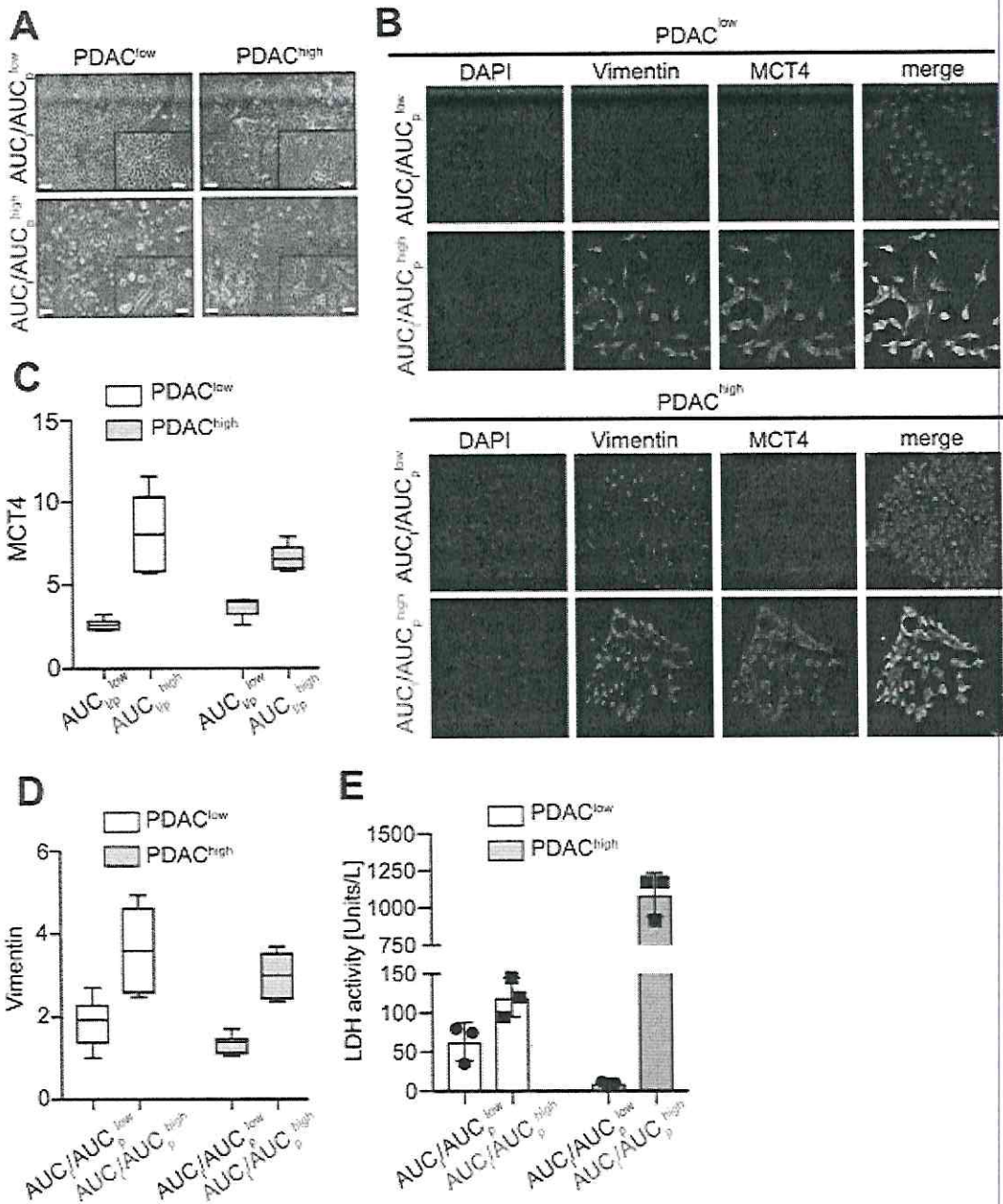
#### References

- [1] Collisson EA, Sadanandam A, Olson P, *et al.* Subtypes of pancreatic ductal adenocarcinoma and their differing responses to therapy. *Nat Med* 2011;17:500-3.
- [2] Karasinska JM, Topham JT, Kalloger SE, *et al.* Altered Gene Expression along the Glycolysis-Cholesterol Synthesis Axis Is Associated with Outcome in Pancreatic Cancer. *Clin Cancer Res* 2020;26:135-146.
- [3] Daemen A, Peterson D, Sahu N, *et al.* Metabolite profiling stratifies pancreatic ductal adenocarcinomas into subtypes with distinct sensitivities to metabolic inhibitors. *Proc Natl Acad Sci U S A* 2015;112:E4410-7.
- [4] Baek G, Tse YF, Hu Z, *et al.* MCT4 defines a glycolytic subtype of pancreatic cancer with poor prognosis and unique metabolic dependencies. *Cell Rep* 2014;9:2233-49.
- [5] Mayer M, Heid I, Topping GJ, *et al.* Metabolic imaging-based subtype prediction in orthotopically transplanted murine pancreatic ductal adenocarcinoma. European Molecular Imaging Meeting, EMIM 2020.



#### CSI with HP[1- $^{13}$ C]pyruvate detects metabolic heterogeneity of mPDAC in vivo.

**A:** Axial  $T_2$ -w abdominal images, HP[1- $^{13}$ C]pyruvate and HP[1- $^{13}$ C]lactate images at peak (25 s, 5 frames) and their metabolite time courses of mPDAC. **B:** Respective automated analysis mask of MCT4 (IHC) staining divided by median, scale bar 100  $\mu\text{m}$ . **C:** Spearman's correlations of  $AUC_i/AUC_p$  ratios and MCT4 expression. **D:** H&E stains of PDAC<sup>low</sup> and PDAC<sup>high</sup> tumors. Scale bar 200  $\mu\text{m}$ . **E, F:** PDAC<sup>low</sup> and PDAC<sup>high</sup> subgroup comparison of mean ADC (**D**) and  $AUC_i/AUC_p$  (**E**) values. Blue and red dots represent tumors from which  $AUC_i/AUC_p^{\text{low}}$  (blue) and  $AUC_i/AUC_p^{\text{high}}$  (red) primary cell lines were derived.



**MCT4 expression correlates with classical and QM phenotype in primary tumor cell lines of mPDAC.**

**A:** Transmitted light microscopy images of cell lines derived from AUC/AUC<sub>p</sub><sup>low</sup> (blue) and AUC/AUC<sub>p</sub><sup>high</sup> (red) tumors. Note cuboid and elongated shape of AUC/AUC<sub>p</sub><sup>low</sup> and AUC/AUC<sub>p</sub><sup>high</sup> cells respectively. **B:** Representative images of co-stained immunofluorescence of MCT4 and Vimentin in the AUC/AUC<sub>p</sub><sup>low</sup> and AUC/AUC<sub>p</sub><sup>high</sup> cells. Scale bar 50µm. **C, D:** Quantification of the fluorescent signal in 6 images/cell line for MCT4 (**C**) and Vimentin (**D**) presented as Box-Whisker-Plot of min to max. **E:** LDH enzyme activity analysis in the AUC/AUC<sub>p</sub><sup>low</sup> and AUC/AUC<sub>p</sub><sup>high</sup> cells.